Genetic Fuzzy Classifier and Nonlinear Analysis for Sleep Stage Identification based on Single EEG Signal

Han Gue Jo

The Graduate School of Information

Yonsei University

Department of Medical Information

Genetic Fuzzy Classifier and Nonlinear Analysis for Sleep Stage Identification based on Single EEG Signal

A Master's Thesis

Submitted to the Department of Medical Information

and the Graduate School of Information of Yonsei University

in partial fulfillment of the

Requirements for the degree of

Master of Science

Han Gue Jo

January 2009

This certifies that the master's thesis of Han Gue Jo is approved.

_____

Thesis Supervisor: Sun kook Yoo

_____

Suk kyoon An

_____

Bong gyou Lee

The Graduate School of Information

Yonsei University

January 2009

Contents

List of Figures

List of Tables

Abstract

Genetic Fuzzy Classifier and Nonlinear Analysis for Sleep Stage Identification based on Single EEG Signal

Jo, Han Gue

Dep. of Medical Information
Graduate School of Information
Yonsei University

Soft-computing techniques are commonly used to detect medical phenomena and help with clinical diagnoses and treatment. This thesis proposes a design for a computerized sleep scoring method which is based on a fuzzy classifier and a genetic algorithm (GA). The proposed method was designed with the fuzzy classifier based on the GA using a single electroencephalogram (EEG) signal that detects differences in spectral features. Polysomnography was performed on four healthy young adults (males with a mean age of 27.5 years). The sleep classifier was designed using a sleep record and tested on the sleep records of the subjects. The results show that the genetic fuzzy classifier (GFC) agreed with visual sleep staging approximately 84.6% of the time in detection of wakefulness (WA), shallow sleep (SS), deep sleep (DS), and rapid eye movement (REM) stages.

The change of correlation dimension (D2) and largest lyapunov exponent (L1) over the whole night sleep EEG was also studied. The results show that D2 and L1 decreased from shallow sleep to deep sleep and D2 increased at REM stage.

Keywords - Electroencephalography, sleep stage, genetic algorithms, fuzzy inference system, Chaos, non-linear analysis, correlation dimension, Lyapunov exponents.

Chapter 1

1. Introduction

Identification of an individual's sleep stages is the first step in sleep studies for clinical diagnosis and treatment of sleep disturbances. It is common knowledge that sleep is an essential state of rest and refreshment. Sleepiness, trouble concentrating, and increased risk of accidents are caused by insufficient sleep, which can be better understood by interpreting sleep stages and the sleep cycle.

In 1968, Rechtschaffen and Kales proposed a method of sleep classification (R-K rule) based on visual that requires an electroencephalogram (EEG), electromyogram (EMG), and electrooculogram (EOG) [1]. This has been the standard for sleep staging for approximately 40 years. However, these criteria have intrinsic restrictions. Using this method for sleep classification is very tedious and because of uncertainty between stages, is highly dependent on the observer's expertise. In addition, the sensors around the face restrict the recording of natural sleep states. Thus, investigators have attempted to use fewer electrodes around the face to address these problems [2-5]. However, the resulting sleep staging systems are not good enough to replace the established R-K rule.

Recent research has investigated differences between individual characteristics in the interpretation of sleep physiology [6-8]. A clear distinction has been found between high within-subject similarity and low between-subject similarity. This suggests that the spectral features recorded during human sleep reflect the traits of each individual [8]. These studies provide evidence that individual differences must be considered in sleep staging.

Therefore, this thesis introduces an automated sleep staging method tailored to each subject which uses fewer electrodes, reduces the intrinsic drawbacks of the former sleep staging method, and improves the performance of computer-based sleep staging systems. The fuzzy inference

method attempts to classify the ambiguous features of sleep stages and is optimized for individual characteristics based on a Genetic algorithm (GA) method. The tuning of the membership function and the number and structure of the fuzzy rules are determined using the training set without any prior knowledge. The spectral features from a single EEG signal are used to train and validate the classifier.

The theory of non-linear dynamic systems, also called 'chaos theory', has now progressed to a stage, where it becomes possible to study self-organization and patter formation in the complex neuronal networks of the brain [9]. The chaotic process, correlation dimension (D2) and largest lyapunov exponent (L1), were performed to quantify the complexity of physiological phenomena at different sleep stages. These results of non-linear analyses would support the differences of sleep EEG at different sleep states.

In the next section, the theoretical background and basic concept of algorithms used in this paper are presented. In the third section, data acquisition and preprocessing methods are presented before explaining the mechanism of the Genetic Fuzzy Classifier (GFC). The fourth stage presents the experimental results of individual differences, performance and nonlinear analysis. In the fourth and last section, the current work is discussed.

Chapter 2

2. Theoretical background

2.1 Sleep EEG

States of brain activity during sleep result from different activations, and inhibiting forces are generated within the neurons of the brain. The sleep EEG is a non-stationary signal with typical changes as a function of the non-REM and REM sleep cycle. Non-REM is further subdivided into four stages of 1(drowsiness), 2(light sleep), 3(deep sleep), and 4(very deep sleep).

Each sleep stage has a dominant pattern that is distinguishable between sleep stages as shown in figure 2.1. Stage 1 occurs most often in the transition from wakefulness to the other sleep stages. During nocturnal sleep, stage 1 tends to be relatively short, ranging from about 1 to 7 min. Stage 1 is defined by a relatively low voltage, mixed frequency EEG with a prominent activity in the 2-7 Hz range. Also during the latter portions of the stage, vertex sharp waves may appear, often in conjunction with the high amplitude 2-7 Hz activity.

Stage 2 is defined by the presence of sleep spindles and/or K complexes and the absence of sufficient high amplitude, slow activity defined in the presence of stages 3 and 4. The presence of a sleep spindle should not be defined unless it is of at least 0.5 sec duration. K complexes are defined as EEG wave forms having a well delineated negative sharp wave which is immediately followed by a positive component.

Stage 3 is defined by an EEG record in which at least 20% but not more than 50% of the epoch consists of waves of 2 Hz or slower which have amplitudes greater than 75 uV from peak to peak. In this stage, sleep spindles may or may not be present.

Stage 4 is defined by an EEG record in which more than 50% of the epoch consists of waves of 2 Hz or slower which have amplitudes greater than 75 uV peak to peak. Most stage 4 epochs have the appearance of being completely dominated by this activity.

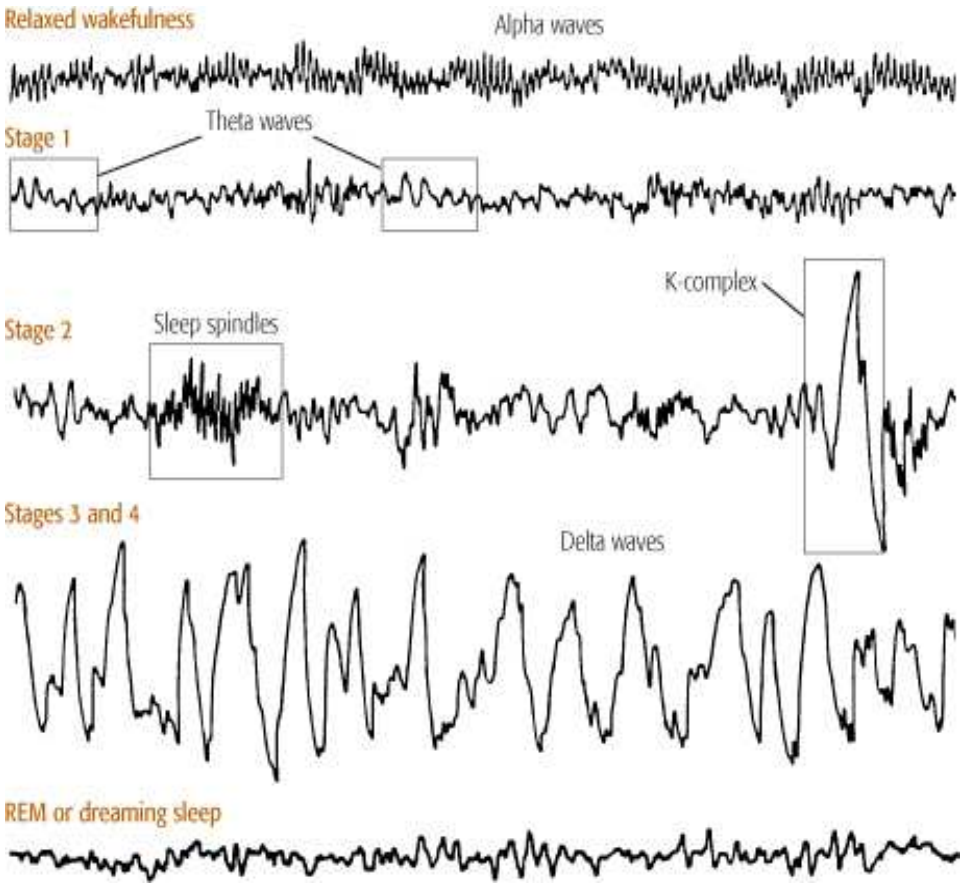

Figure 2.1 Common characteristic of each sleep stages

Stage REM is defined by the concomitant appearance of relatively low voltage, mixed frequency EEG activity and episodic rapid eye movements (REMs). The EEG pattern resembles the one described for stage 1, except that vertex sharp waves are not prominent in stage REM. Also, in stage REM distinctive 'saw-tooth' waves frequently, but not always, appear in vertex and frontal regions in conjunction with bursts of REM.

2.3 Fuzzy inference system

Fuzzy inference method is one of the soft-computing techniques that are in use to classify for uncertainties which was introduced by Zadeh in 1965[10]. Fuzzy theory deals with sets or categories whose boundaries are blurry or, in other words, "fuzzy". It is an algorithm that infers the results from the fuzzy sets and a set of fuzzy rules. Fuzzy sets are identified by membership functions that allow various degrees of the elements of the given input set. The fuzzy rules are applied to the multi-variable fuzzy sets and converged to a class label in one of the results.

2.4 Genetic Algorithms (GA)

GA was proposed in 1975 by Holland. It is a searching algorithm to solve an optimization problem based on natural selection [11]. To precede a GA, the parameters of the solution must be encoded into a numerical stream that is called a chromosome. The purpose of GA is to find the appropriate chromosome by reconstruction of chromosomes from a population. First, GA randomly generates a certain number of chromosomes to form an initial population. This population is considered as a generation.

Second, each chromosome is evaluated by a fitness function that measures the suitability of an individual chromosome in a given environment. The fitness function accounts a decoded chromosome and produces a numerical value as a measure of the performance of the chromosome.

Third, to reconstruct a new generation, reproduction, crossover, and mutation operators are expected to obtain child chromosomes from parent chromosomes. In the process of reproduction, the chromosome with a higher fitness value survives at a higher probability and a lower fitness value survives at a lower probability. Crossover is a process that allows for an

exchange of numerical streams from two chromosomes to produces a new chromosome. The mutation operation involves a probability that arbitrary bits of streams will be changed from their original state. This is done to attempt to find a global optimum rather than a local one and preventing the population of chromosomes from becoming too similar to each other.

This process, along with steps two and three presented above, are sustained until the best chromosome is generated. Finally, the chromosome is decoded into original parameters of solution that solve the problem in optimum.

2.5 Chaotic process

The presence of chaos in a dynamical system is quantified by measuring the complexity of dimension and characteristic exponents which estimate of the level of chaos. Dimension gives an estimate of the system complexity that is solved by correlation dimension (D2). Largest lyapunov exponents (L1) quantify the exponential sensitivity of divergence to initial condition and estimate the amount of chaos in a system.

2.5.1 Phase Space (attractor dynamics)

The first step of chaotic analysis involves reconstructing the phase space from a single time series. Phase space is an abstract mathematical space in which to view the dynamics. This is accomplished by utilizing time delay and embedding dimension. The choice of an appropriate time delay T and embedding dimension d is important for the success of reconstructing the attractor with finite EEG data. For the time delay, T, the first local minimum of the average mutual information between the set of measurements $X(t)$ and $X(t+T)$ was used [12]. Mutual information measures the general dependence of two variables.

The minimum embedding dimension in the reconstruction producer was estimated using an algorithm proposed by Kennel et al [13]. The algorithm is based on the idea that in the passage

from dimension *d* to *d+1*, one can differentiate between points on the orbit that are true neighbors and those that are false. A false neighbor is a point in the data set that is identified as a neighbor solely because of viewing the attracter in too small an embedding space. When the point in the data has achieved a large enough embedding space, all neighbors of every attractor point in the multivariate phase space will be true neighbors.

Mathematically, a reconstructed phase space can be described as follows

$$Y(t) = [X(t),\ X(t+T),\ X(t+2T),\ \ldots,\ X(t+(d-1)T)] \tag{1}$$

where *x(t)* is the time series from a dynamical system, *T* represents appropriate time delay and *d* is a proper embedding dimension for phase space reconstruction as.

2.5.2 Correlation Dimension (D2)

D2 describes the dimensionality of the underlying process in relation to its geometrical reconstruction in phase space. This thesis estimated the complexity using the approach based Grassberger-Procaccia algorithm [14]. It estimates the average number of data points within a radius *r* of the data point r_{ij}. Let *C(r)* be the number of points within all the circles of radius *r*.

$$C(r) = \frac{1}{N(N-1)} \sum_{j=1}^{N} \sum_{i=j+1}^{N} \Theta(r - r_{ij}) \tag{2}$$

where *N* represent the number of points in phase space and Θ is the Heaviside function

$$\Theta(x) = \theta \begin{Bmatrix} 0 \ \ for\ \ x < 0 \\ 1 \ \ for\ \ x \geq 0 \end{Bmatrix} \tag{3}$$

and r_{ij} is the spatial separation between two points labeled *i* and *j*, usually given in an m-dimensional time-delay embedding by Euclidean norm. A plot of $log(C_{(r)})$ versus $log(r)$ should give an approximately straight line whose slope in the limit of small r and large N is the correlation dimension.

$$D_2 = \lim_{r \to 0} \lim_{N \to \infty} \frac{\log C_{(r)}}{\log r} \tag{4}$$

2.5.3 Largest Lyapunov Exponent (L1)

The L1 from the EEG signals was evaluated based on Rosenstein, et.al algorithm [15]. For their method, the L1 can be defined using the following equation

$$d(t) = Ce^{\lambda_1 t} \tag{5}$$

where d(t) is the average divergence at time t and C is a constant that normalizes the initial condition. After reconstructing the phase space, the algorithms find the nearest neighbor of each point in the trajectory. The nearest neighbor, $X_{\hat{j}}$, is found by searching for the point that minimizes the distance to the particular reference point, X_j, This is expressed as

$$d_j(0) = \min_{x_{\hat{j}}} \left\| X_j - X_{\hat{j}} \right\| \tag{6}$$

where $d(0)_j$ is the initial distance from the j^{th} point to its nearest neighbor, and $\|...\|$ denotes the Euclidean norm. By taking the logarithm of both sides of Eq. (5), we obtain

$$\ln d_j(i) = \ln C_j + \lambda_1 (i \cdot \Delta t). \tag{7}$$

where Δt is the sampling period of the time series, and $d_j(i)$ is the distance between the j^{th} pair of nearest neighbors after *i* discrete-time steps, i.e, $i \cdot \Delta t$ seconds. Eq. (7) represents a set of approximately parallel lines (for *j*=1, 2, ... , N), each with a slope roughly proportional to λ_1. The largest lyapunov exponent is calculated using a least-square fit to the average line defined by

$$y(i) = \frac{1}{\Delta t} \left\langle \ln d_j(i) \right\rangle, \tag{8}$$

where $\langle ... \rangle$ denotes the average over all values of *j*.

Chapter 3

3. Materials and methods of GFC

3.1 Data acquisition

Four healthy young men between the ages of 27 and 29 years (mean age, 27.5 years) volunteered to participate in the present study. They did not use any medications and had no sleep complaints. The subjects were asked to go to bed between 10 and 12 pm and were permitted to sleep for a maximum of 8 hours. All recordings were preceded by at least one adaptation night in the sleep laboratory.

Polygraphic recordings of the EEG, EOG, and EMG were obtained. EEG electrodes were placed at C3 and C4, according to the international 10-20 electrode placement guidelines. The ground and reference were placed in the right earlobe. The chin EMG was recorded at the submental region. The EOG leads were placed on the outer canthus of the left and right eyes. For the recording, the BIOPAC MP150 system was used with a 1,000 Hz sampling rate and a gain of 10,000. The high pass filter was set to 0.5 Hz and the low pass filter to 100 Hz. The 60 Hz notch filter was on at all times. All subjects gave written informed consent prior to the experiments.

Sleep stages were scored visually on a computer screen using standard criteria for each 30 second epoch. In this study, the sleep stages were divided into four stages (wakefulness: WA, shallow sleep: SS, deep sleep: DS, and REM). Because Stage 1 is a transient state, Stage 1 and Stage 2 together were classified as shallow sleep (SS). Sleep Stages 3 and 4 were called deep sleep (DS). Table 3.1 shows the data sets from the four subjects. The data from each subject were divided into training and validation sets.

Table 3.1 The recording data sets of each subject

subjects	recording sets		WA [epochs]	SS [epochs]	DS [epochs]	REM [epochs]	Total [epochs]
A	A1	training	18	436	127	195	776
	A2	validation	269	461	111	101	942
	A3		37	378	111	187	713
B	B1	training	31	332	90	125	578
	B2	validation	70	360	101	52	583
	B3		25	364	121	221	731
C	C1	training	10	117	172	39	338
	C2	validation	7	308	207	215	737
	C3		201	336	195	145	877
D	D1	training	6	252	181	139	578
	D2	validation	13	249	77	142	481

3.2 Data preprocessing

The Fast Fourier Transform (FFT) algorithm was performed without artifact rejection on a single EEG signal, C3-A2, after consecutive 30 seconds epochs. The length of the Hanning window for FFT was 32,768. Power spectra were obtained for the following bandwidths: delta (1-4 Hz), theta (4-7.5 Hz), alpha (7.5-12 Hz), sigma (12-14 Hz), and beta (16-25 Hz).

Relative powers for each of the epochs were computed as (power per bandwidth) / (total power) where the total power was calculated by summing the power for every five bandwidths per epoch. To obey the "three minute rule" of sleep staging criteria [1], the epochs were represented as the median values of six periods in sequence (6 periods*30 s = 3 min). After

mediation, the relative power values of a record were normalized between 0 and 1 and applied as input sets to the fuzzy classifier.

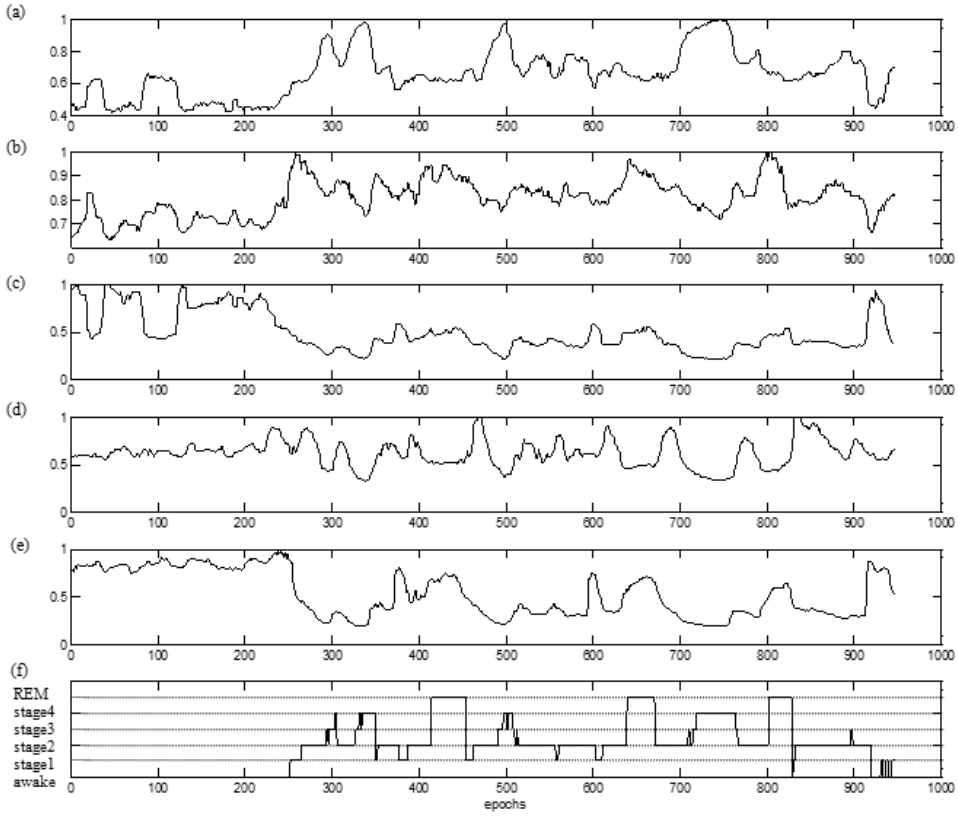

Figure 3.1 An example of normalized relative power and sleep stages for a subject: (a), (b), (c), (d), and (e) are the normalized relative power of delta, theta, alpha, sigma, and beta respectively; (f) classified stages by means of R-K rule

Figure 3.1 shows the normalized relative powers of delta, theta, alpha, sigma, and beta with the sleep stages for a subject. It is evident from this figure that a great amount of pattern variability exists within a single stage. The delta frequency during deep sleep showed a significantly higher percentage of power than the other frequencies. The alpha bandwidth appeared to be related to WA, and beta showed more REM and WA signals than the other stages.

There were also significant differences between theta and sigma in the REM and SS stages. Theta activity was present in the REM stage, and sigma activity was present in the SS stage. These frequency characteristics present differently between inter-subjects (refer to 4.1).

3.3 Model of the fuzzy classifier

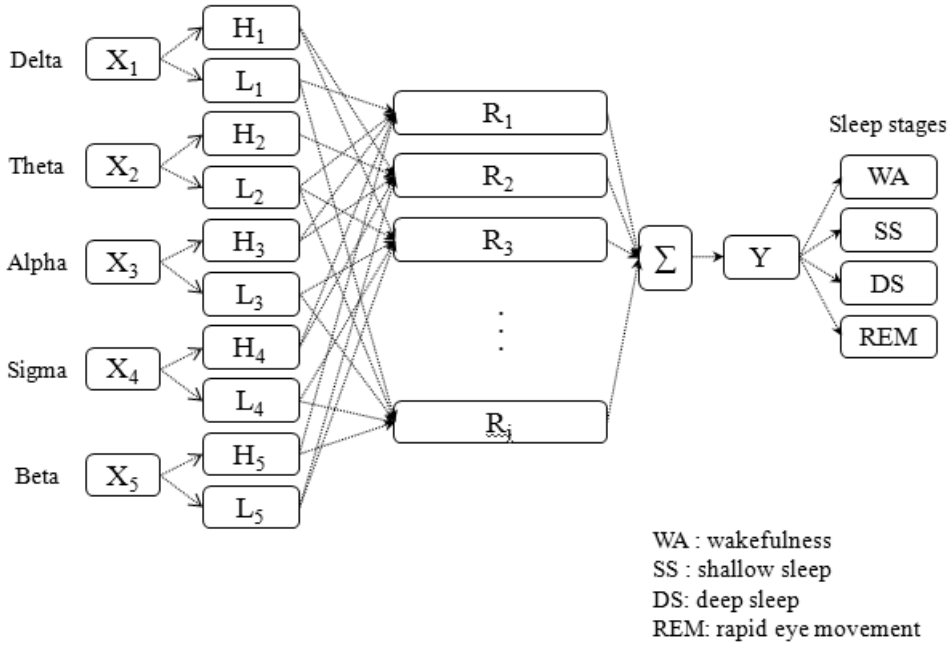

Figure 3.2 Structure of Mamdani fuzzy classifier applied to the sleep identification

A common type of fuzzy logic control called a Mamdani was applied to this study [10]. Figure 3.2 shows how the structure of the Mamdani-type fuzzy classifier is applied to sleep identification. This system has five input sets X_i (i=1, 2, ..., 5), one output set Y, and j fuzzy rules. Y denotes the universal output set that would be defuzzified to the objective values *WA*, *SS*, *DS*, or *REM*. Input X_i is divided into two fuzzy sets, H_i and L_i, which denote the higher and lower percentage in linguistic terms, respectively. The input fuzzy sets can be expressed as

$$L_i = \{x_i, uL_i(x_i) \mid x_i \in X_i\}, \tag{9}$$

$$H_i = \{x_i, uH_i(x_i) \mid x_i \in X_i\}, \tag{10}$$

where x_i are the elements of input set X_i. The functions $uH_i(x_i)$ and $uL_i(x_i)$ are the membership functions of x_i in X_i, and are associated with a given set X_i that maps x_i to its appropriate membership grade between 0 and 1. The grade of the membership functions can be written as

$$uL_i(x_i) = \begin{Bmatrix} 1 & , \ x_i \le w_i^1 \\ -\frac{x_i}{w_i^2} + \frac{1-w_i^3}{w_i^2} & , \ w_i^1 < x_i \le 1-w_i^3 \\ 0 & , \ w_i^3 - 1 < x_i \le 1 \end{Bmatrix}, \tag{11}$$

$$uH_i(x_i) = \begin{Bmatrix} 0 & , \ x_i \le w_i^1 \\ \frac{x_i}{w_i^2} - \frac{w_i^1}{w_i^2} & , \ w_i^1 < x_i \le 1-w_i^3 \\ 1 & , \ w_i^3 - 1 < x_i \le 1 \end{Bmatrix}. \tag{12}$$

While w_i^1 and w_i^3 denote the low and high periods respectively, w_i^2 represents the boundary of the transition period between low and high (Fig. 3.3). The determination of w_i^1, w_i^2, and w_i^3 sets the boundary and scope of the membership functions which affect the boundary between the high and low of input set X_i.

To design Mamdani fuzzy logic, the linguistic terms H_i and L_i can be combined in rules to form an inference system. Rule R_j is written as

If (X_1 *is* A_1 *and* X_2 *is* A_2 *... and* X_i *is* A_i) *Then* (Y *is* B_j), (13)

where A_i is associated with one of the fuzzy sets of the fuzzy partition (H_i or L_i) for X_i in the antecedent part, and B_j represents one of the fuzzy sets of the fuzzy partition (*WA*, *REM*, *SS*, or *DS)* for Y in the consequent part. In the antecedent part, there are *i* input sets with two linguistic terms that can display 2^i possible rules, and each rule must be assigned to one of the output fuzzy sets. The assignment of each rule to one of the output fuzzy sets and the generation of a set of fuzzy rules determine the fuzzy inference system.

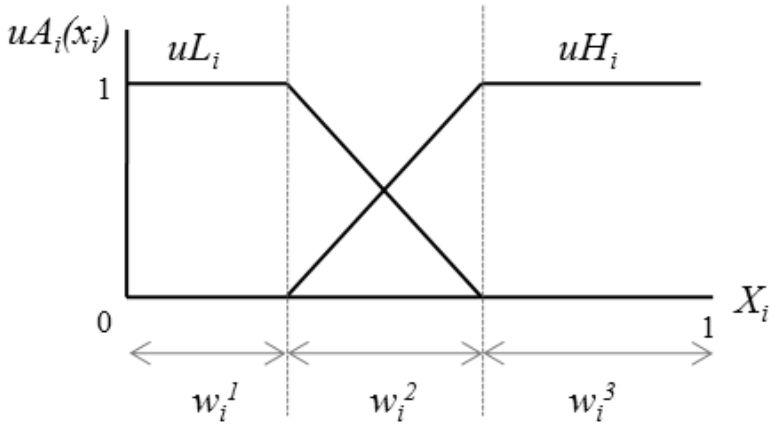

Figure 3.3 Two membership functions of an input set

After a suitable fuzzy rule set is generated, the antecedent part of each rule is calculated by a fuzzy conjunction which is reshaped into a fuzzy set in the consequent part. When the antecedent parts of each rule are calculated, the fuzzy disjunction is calculated to aggregate the consequents. These operations can be calculated as follows:

fuzzy conjunction:

$$uB_j(y) = \min[u_{A_1}(x_1), u_{A_2}(x_2), \ldots, u_{A_i}(x_i)], \tag{14}$$

where $uB_j(y)$ denotes the results of implication that represent the output of rule *j* and are combined into an output variable.

fuzzy disjunction:

$$u(y) = \max[uB_1(y), uB_2(y), \ldots, uB_j(y)], \tag{15}$$

where $u(y)$ denotes the results of aggregation that represent the output variables of each rule and are combined into a single fuzzy set.

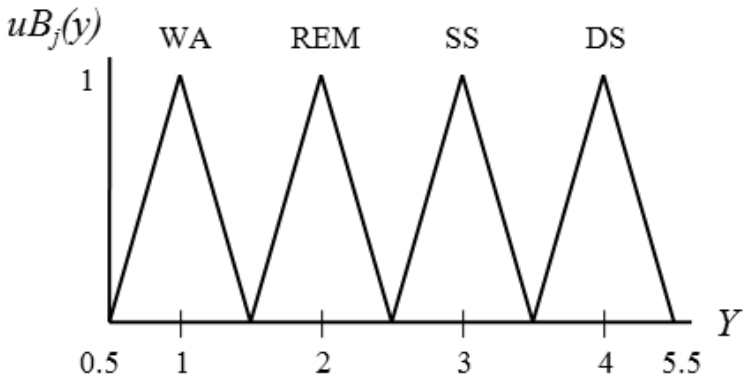

Figure 3.4 Four fuzzy sets of the output set

The crisp output of a fuzzy classifier can be evaluated by defuzzification of $u(y)$. This study performed the middle of the maximum defuzzification method which represents the mean value of all local membership functions reaching the maximum. A sleep stage was determined as being awake when the crisp output value was 1, rapid eye movement when the value was 2, shallow sleep when the value was 3, and deep sleep when the value was 4 (Fig. 3.4).

3.4 GA solution

The problem of designing a fuzzy classifier can be expressed as finding the grade of the membership functions and a set of fuzzy rules that achieve stability according to the given conditions. Hence, the GA was built to determine the parameters of the membership functions and a set of fuzzy rules.

3.4.1 Chromosome representation

The structure of a GFC chromosome is composed of two binary-coded sequences that define the grade of membership function **C** and a set of fuzzy rules **S**. **C** can be written as

$$\mathbf{C} = (C_{11}, C_{21}, C_{31}, C_{12}, C_{22}, C_{32}, \ldots , C_{1i} , C_{2i} , C_{3i}), \tag{16}$$

where C_{1i} , C_{2i} , and C_{3i} represent the periods w_i^1, w_i^2, and w_i^3 of input set X_i in binary code, respectively (Fig. 3.3). The length of w_i^l is formulated as

$$w_i^l = \frac{C_{li}}{C_{1i} + C_{2i} + C_{3i}}, \tag{17}$$

where l=1, 2, and 3 denote the high, low, and transition periods of X_i.

A set of fuzzy rules sequence **S** is expressed as

$$\mathbf{S} = (S_{11},S_{21},S_{12},S_{22}, .. ,S_{1n},S_{2n},S_{31},S_{32}, \ldots ,S_{3n}), \tag{18}$$

where n denotes the number of possible rules from the antecedent parts, and S_{1n} and S_{2n} represent the output variables of rule n (Table 3.2). S_{3n} defines a set of rules which denotes the presence of rule '1' or not '0' for n rules.

Table 3.2 Representation of sleep stages

Chromosome		sleep stages
S_{1n}	S_{2n}	
0	0	WA
0	1	REM
1	0	SS
1	1	DS

3.4.2 Fitness function

One of the most important considerations in the successful generation of a GA is the design of the fitness function. The design of the system must be appropriate for the desired sleep stage values. This study considers the fitness function to be the mean error rate of the four sleep stages. This can be formulated as

$$fitness = (1 - \frac{1}{m}\sum_{K=1}^{m}\frac{TP}{N})^2 \tag{19}$$

where *TP* denotes the number of sleep stages that are correctly measured, *N* represents the length of a sleep stage, and *K*=1, 2, 3, or 4 indicates one of the sleep stages, *WA*, *REM*, *SS*, or *DS*, respectively.

3.4.3 GA parameters

The GA was generated with a population size of 20, 50 generations, and 2 as the elite rate that retains the two best populations for the next generation. This study used a roulette wheel to

reproduce chromosomes in a process which allows chromosomes with larger fitness values to have higher probabilities that larger numbers of their copies will exist in the next generation. A scatter function was used to cross the genes of the two parents with a 0.8 crossover rate. This created a random binary vector in which the gene from the first parent was obtained at '1' and from the second parent at '0', and the genes were combined to form a child gene for the new generation. Gaussian mutation, chosen from a Gaussian distribution, was applied to mutate the parent genes. The amount of mutation, which is proportional to the standard deviation of the distribution, decreases linearly at each new generation, finally to 0 at the final step.

In the chromosome representation, a period of w_i^l was encoded in 5 bits, C_{li}, which reveal 75 bits, **C,** for the five input sets. Based on the assumption of two fuzzy sets per input X_i, as is the case with i=5 inputs, there were $n=2^5=32$ possible rules, and each rule was assigned to one of the output variables represented by S_{1n} and S_{2n}. Then, a set of fuzzy rules from the n possible rules was corrected by S_{3n}. Consequently, the chromosome was expressed as 171 bits, representing an optimized membership function (75 bits) and fuzzy rules selection (96 bits).

Chapter 4

4. Results

4.1 Individual differences

Figure 4.1 presents intra- and inter-subject differences and similarities found during the tests. The bars indicate the mean normalized relative power of the five frequency bands for all epochs in each sleep stage. Error bars represent the standard deviation. Significant differences between individual subjects occurred in the alpha, sigma, and beta bands, whereas the theta band did not show any significant differences. At delta frequencies, the individual differences occurred in the REM stage. The differences between individual subjects are shown in the WA and DS stages of the sigma band, and in the REM stage of the alpha band. The beta band also displayed individual differences in the DS stage. The SS and DS stages showed similarities between subjects in delta band, the WA stage showed similarities in the alpha and beta frequencies, and the SS stage showed similarities at the sigma frequencies.

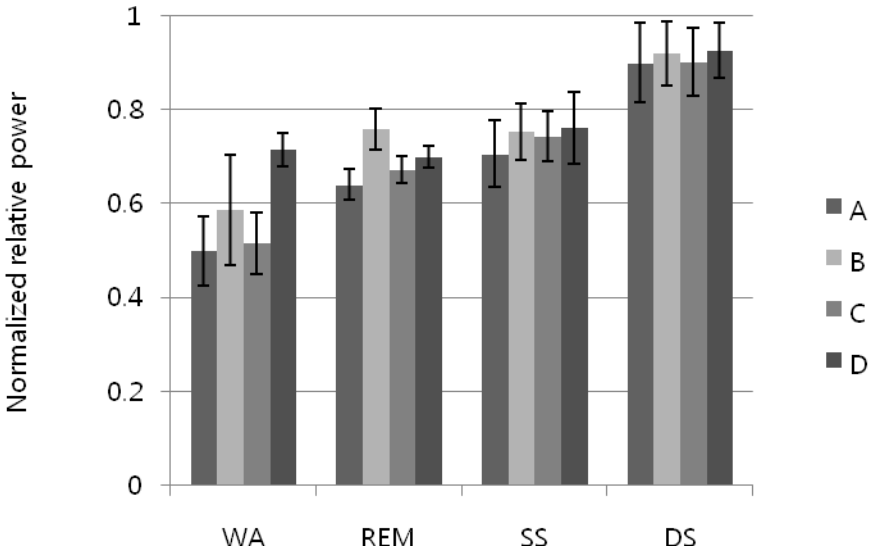

(A) Normalized relative power of delta range

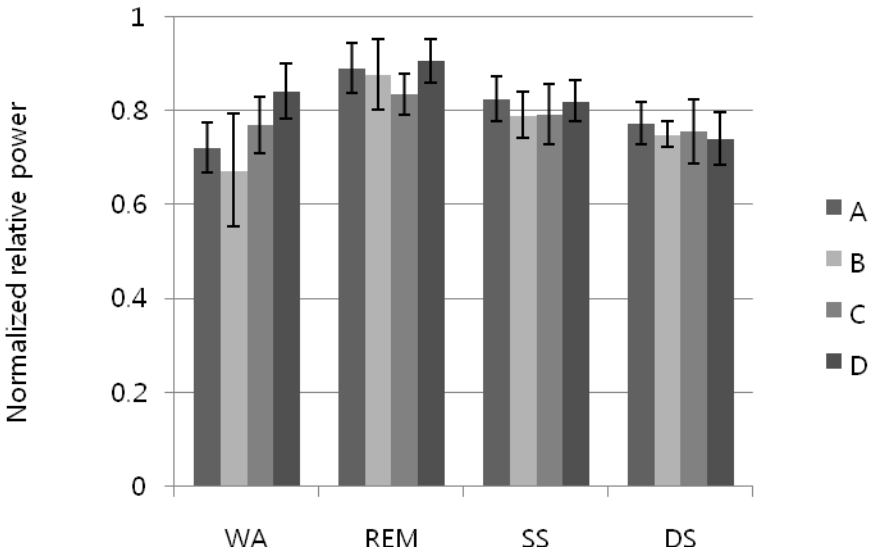

(B) Normalized relative power of theta range

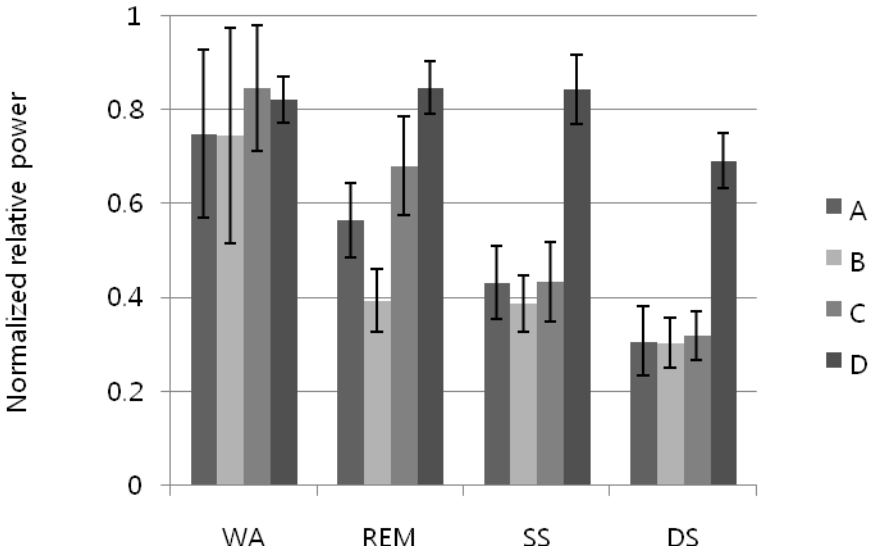

(C) Normalized relative power of alpha range

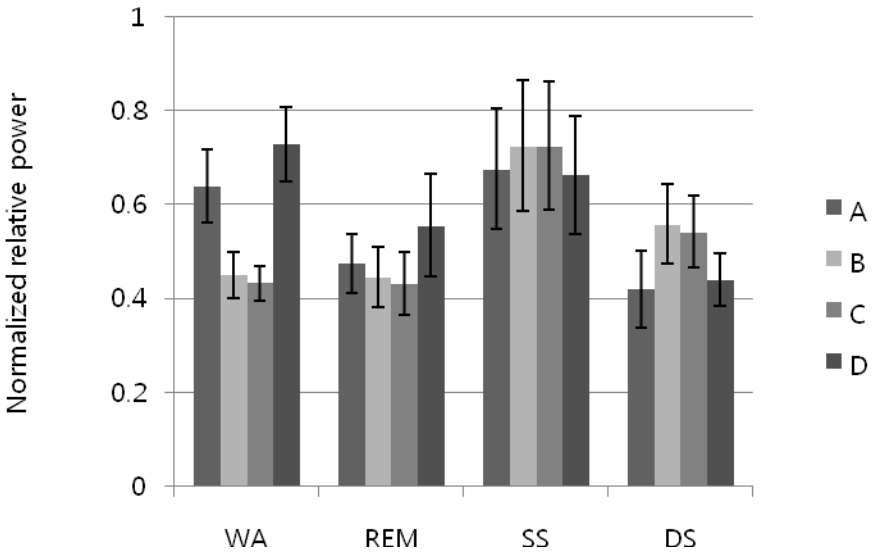

(D) Normalized relative power of sigma range

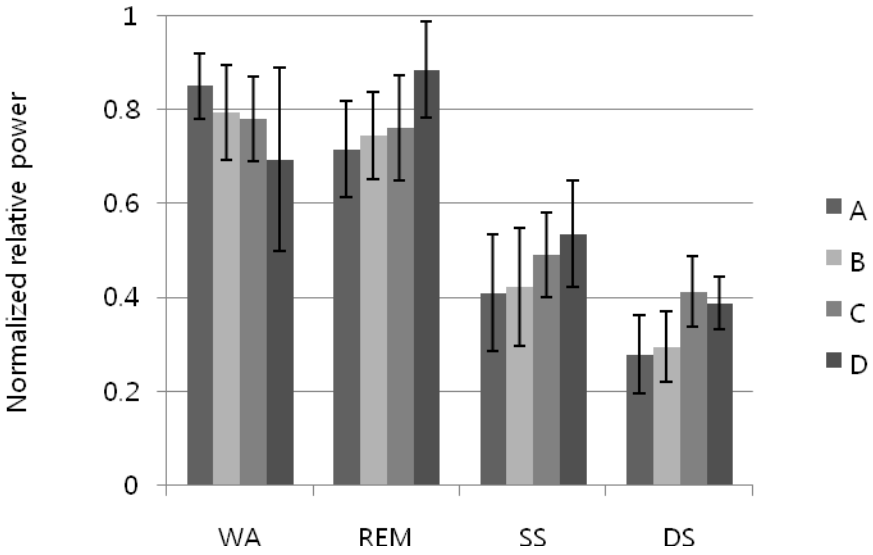

(E) Normalized relative power of beta range

Figure 4.1 Individual differences from normalized relative power of five frequency band in subsequent sleep stages.

4.2 GFC Performance evaluation

The performance of the system was measured using the following equations.

$$Sensitivity = \frac{TP}{TP + FN} \times 100 \ , \tag{20}$$

$$Specificity = \frac{TN}{TN + FP} \times 100 \ , \tag{21}$$

Table 4.1 Agreement of GFC scoring and visual scoring

subjects	GFC / visual	WA	SS	DS	REM	Sensitivity
A	WA	298	2	0	8	96.8%
	SS	54	721	51	13	86.0%
	DS	0	41	178	3	80.2%
	REM	25	25	0	238	82.7%
	Specificity	79.0%	91.4%	77.7%	90.8%	
	Accuracy					86.6%
B	WA	76	0	1	18	80.0%
	SS	11	596	45	72	82.3%
	DS	0	40	180	2	81.1%
	REM	12	12	2	247	90.5%
	Specificity	76.8%	92.0%	78.9%	72.9%	
	Accuracy					83.6%
C	WA	162	39	0	7	77.9%
	SS	0	548	65	31	85.1%
	DS	0	49	347	6	86.3%
	REM	0	57	0	303	84.2%
	Specificity	100%	79.1%	84.2%	87.3%	
	Accuracy					84.3%
D	WA	3	10	0	0	23.1%
	SS	4	196	35	14	78.7%
	DS	0	4	73	0	94.8%
	REM	0	21	0	121	85.2%
	Specificity	42.9%	84.8%	67.6%	89.6%	
	Accuracy					81.7%
total	WA	542	51	1	33	86.4%
	SS	69	2061	196	130	83.9%
	DS	0	134	778	11	84.3%
	REM	37	115	2	909	85.5%
	Specificity	83.6%	87.3%	79.6%	83.9%	
	Accuracy					84.6%

where *TP*, *FN*, *TN*, and *FP* denote true positive, false negative, true negative, and false positive, respectively. *TP* represents the number of sleep stages that are correctly labeled as a desired sleep stage, and *FN* denotes the number of sleep stages that are incorrectly labeled as

non-desired sleep stages by GFC. *TN* is the number of sleep stages that are correctly labeled as non-desired sleep stages, and *FP* expresses the number of sleep stages that are incorrectly labeled as desired sleep stages by GFC.

As shown in Table 4.1, the classifier identified the correct sleep stage with a mean accuracy of 84.6% and in the range from 81.7% to 86.6%. The total average sensitivity was approximately 85.0% in the range from 83.9% to 86.4%, and it had an average specificity of about 83.6% in the range from 79.6% to 87.3%.

4. 3 Nonlinear analysis

Before quantifying the chaotic phenomena, the algorithm was verified by well-known chaotic systems. Table 4.2 summarizes the chaotic dynamic systems primarily examined in this study for D2 and L1. The mean error for calculation of chaotic systems was less than 4% ranged 0.29~8.83% as shown in table 4.3.

Figure 4.2 represents the mean D2 and the sleep stages for entire sleep EEG of each sleep recording sets where error bars denote the standard deviation. The most significant finding is the decrease of mean D2 from shallow sleep (Stage1 and 2) to deep sleep (Stage3 and 4) and increased at REM sleep stage. The differences between individual subjects are displayed in WA stage.

Table 4.2 Chaotic dynamical systems with theoretical values for the D2 and L1

Chaotic System	Equations	parameters	Δt	expected	
				D2	L1
Logistic	$x_{i+1} = a x_i (1 - x_i)$	$a = 4.0$	1	1.0	0.693
Henon	$x_{i+1} = 1 - a x_i^2 + y_i$ $y_{i+1} = b x_i$	$a = 1.4$ $b = 0.3$	1	1.220	0.419
Lorenz	$\dot{x} = \sigma(y - x)$ $\dot{y} = x(R - z) - y$ $\dot{z} = xy - bz$	$\sigma = 10.0$ $R = 28.0$ $b = 8/3$	0.01	2.068	0.906
Rossler	$\dot{x} = -y - z$ $\dot{y} = x + ay$ $\dot{z} = b + z(x - c)$	$a = 0.20$ $b = 0.20$ $c = 5.70$	0.1	1.991	0.071

Δt : Sampling period of time series

Table 4.3 Experimental results for chaotic systems for D2 and L1

Chaotic System	expected		calculated		% error	
	D2	L1	D2	L1	D2	L1
Logistic	1.0	0.693	0.977	0.691	2.30	0.29
Henon	1.220	0.419	1.207	0.434	1.07	3.58
Lorenz	2.068	0.906	1.946	0.986	5.89	8.83
Rossler	1.991	0.071	1.944	0.069	2.36	2.82

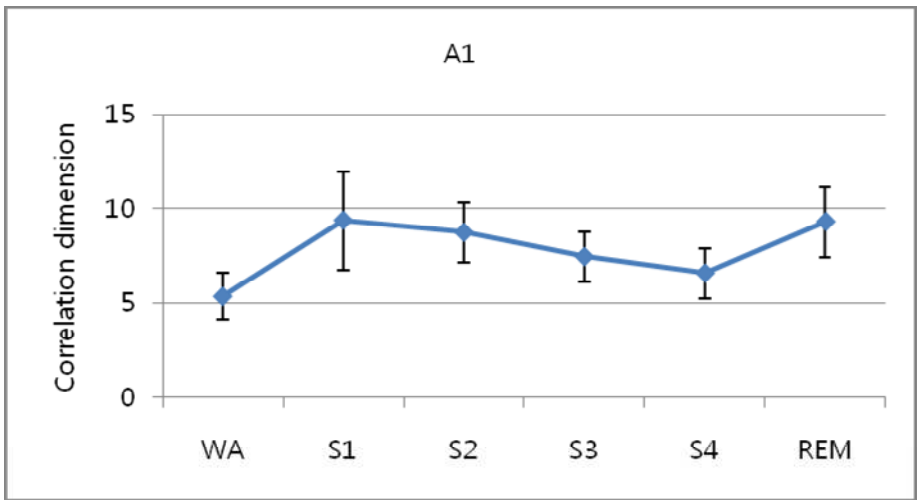
A1
Correlation dimension
15
10
5
0
WA
S1
S2
S3
S4
REM

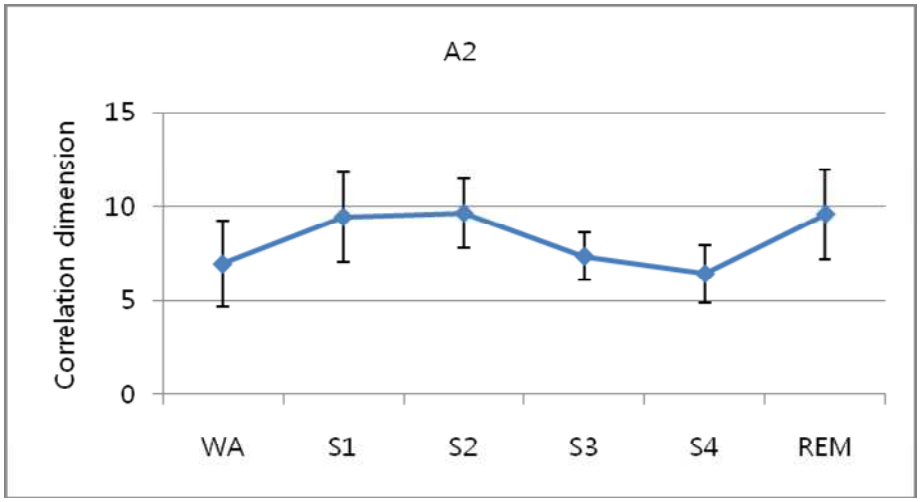
A2
Correlation dimension
15
10
5
0
WA
S1
S2
S3
S4
REM

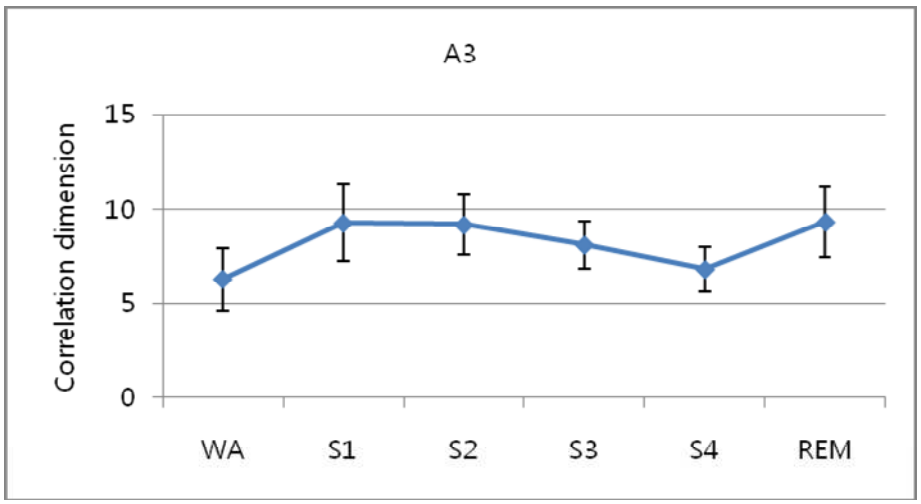
A3
Correlation dimension
15
10
5
0
WA
S1
S2
S3
S4
REM

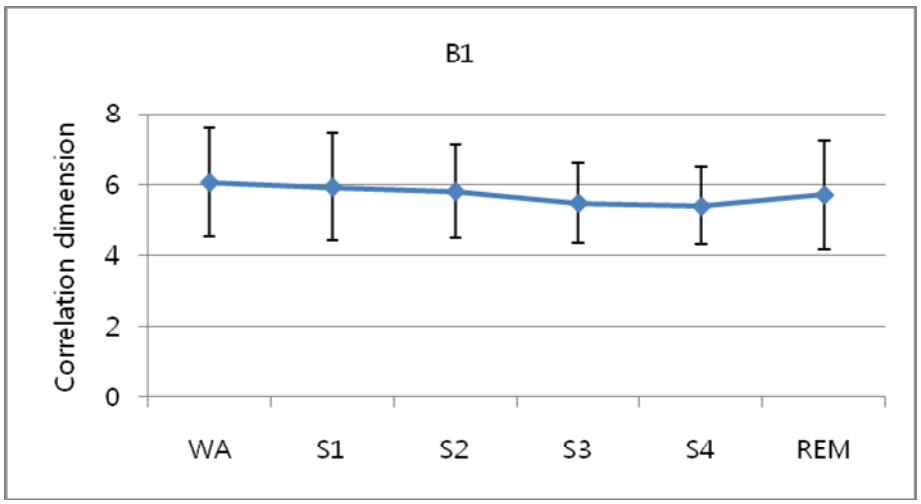
B1
Correlation dimension
8
6
4
2
0
WA
S1
S2
S3
S4
REM

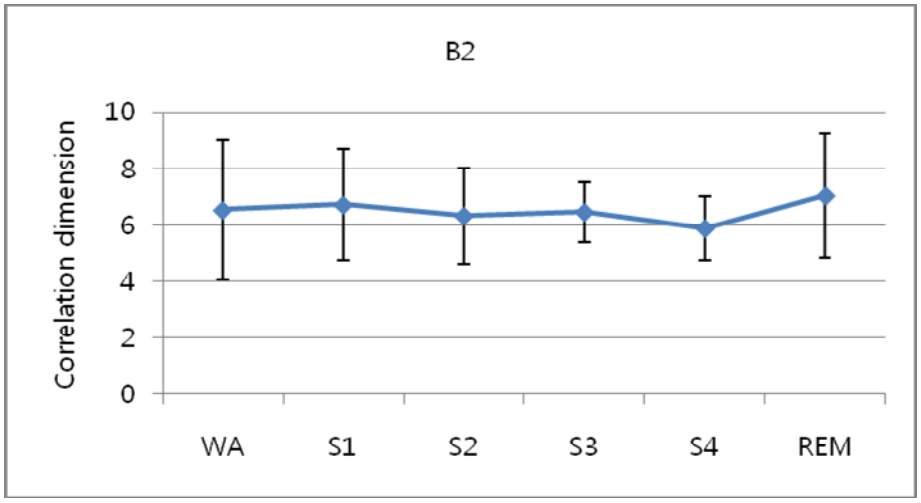
B2
Correlation dimension
10
8
6
4
2
0
WA
S1
S2
S3
S4
REM

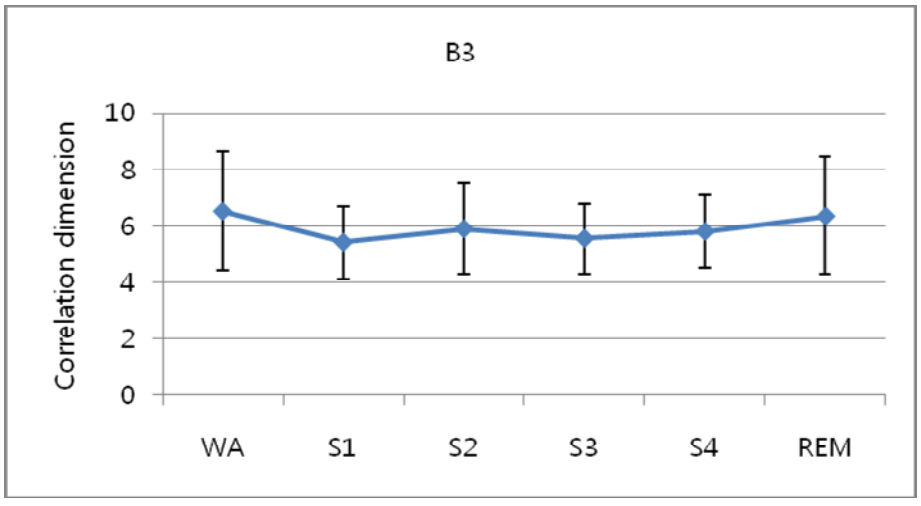
B3
Correlation dimension
10
8
6
4
2
0
WA
S1
S2
S3
S4
REM

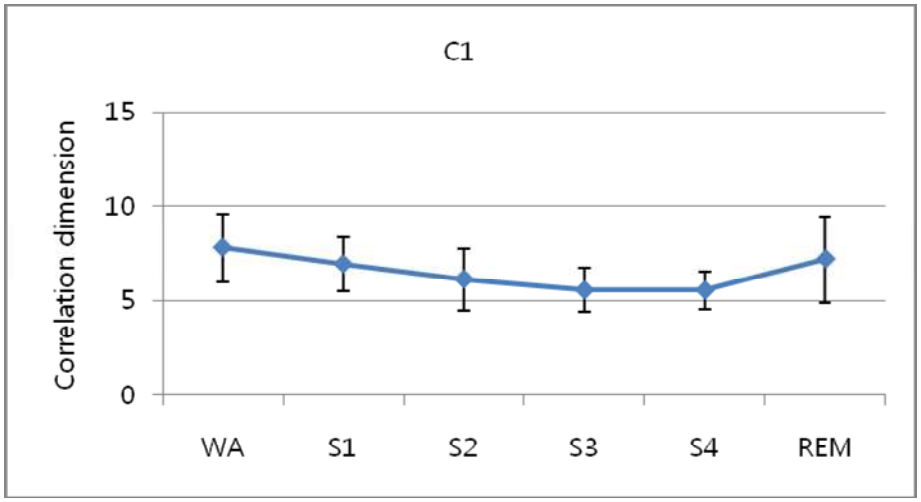
C1
Correlation dimension
15
10
5
0
WA
S1
S2
S3
S4
REM

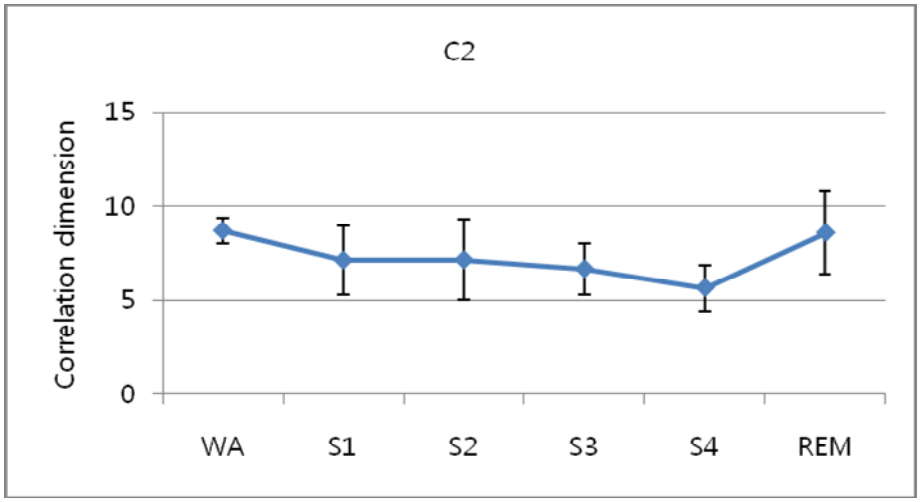
C2
Correlation dimension
15
10
5
0
WA
S1
S2
S3
S4
REM

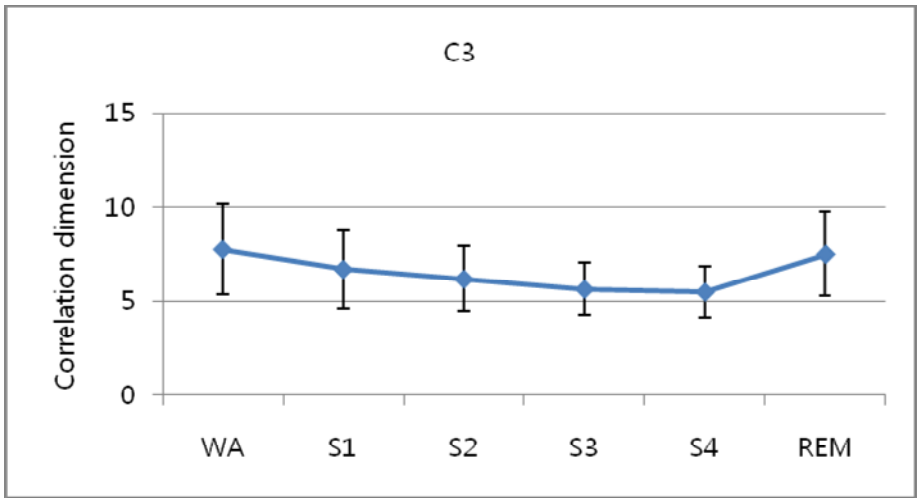
C3
Correlation dimension
15
10
5
0
WA
S1
S2
S3
S4
REM

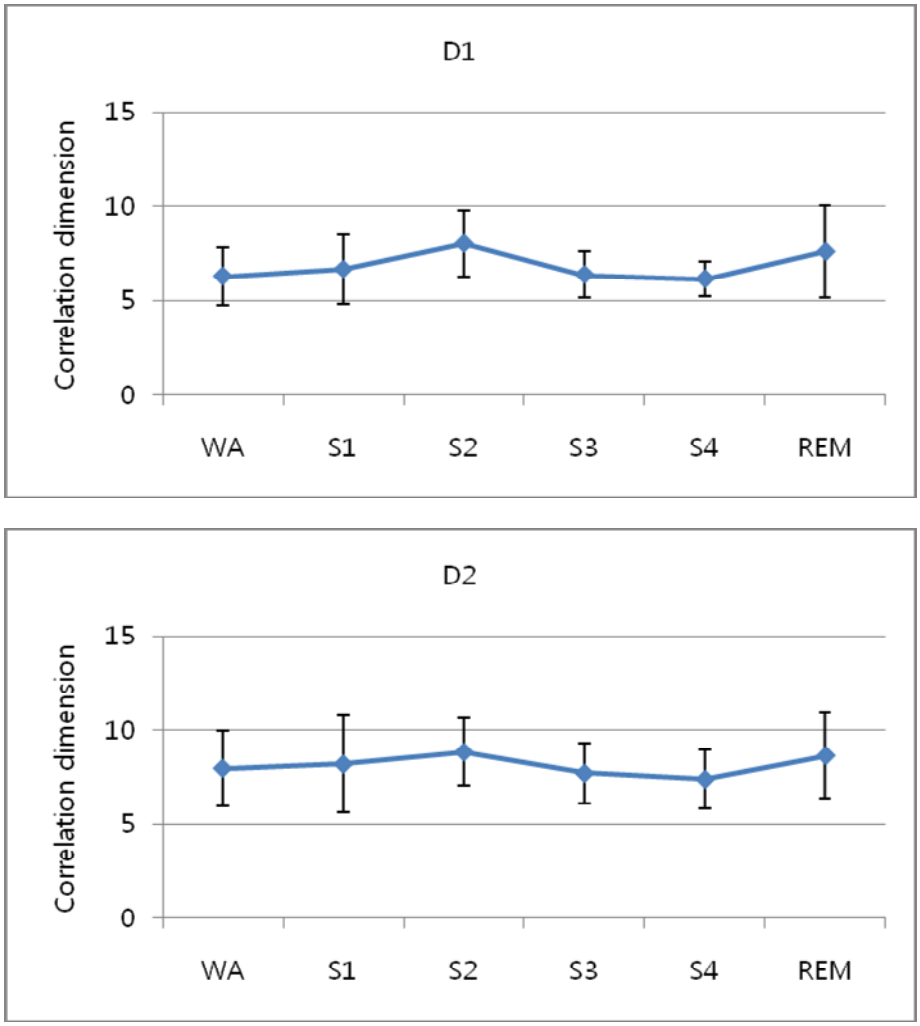

Figure 4.2 Mean and S.D. of D2 for WA stage, sleep stage 1, 2, 3, 4, and REM stage for each recording sets

The mean values and standard deviations of *L1* are shown in figure 4.3. The results show that the more sleep moves to DS (Stage3 and 4), the lower *L1*. Figure 4.2 and 4.3 displayed a similar pattern of *D2* and *L1* in entire sleep stages between and within-subjects.

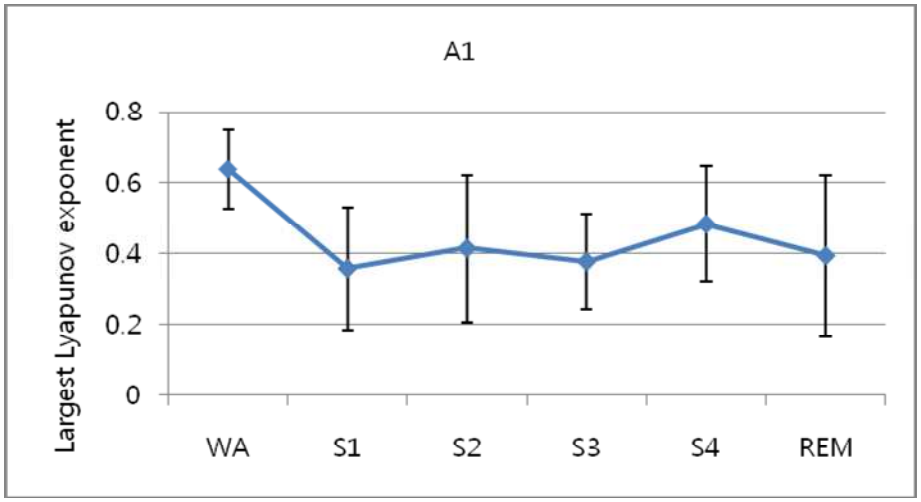
A1
Largest Lyapunov exponent
0.8
0.6
0.4
0.2
0
WA
S1
S2
S3
S4
REM

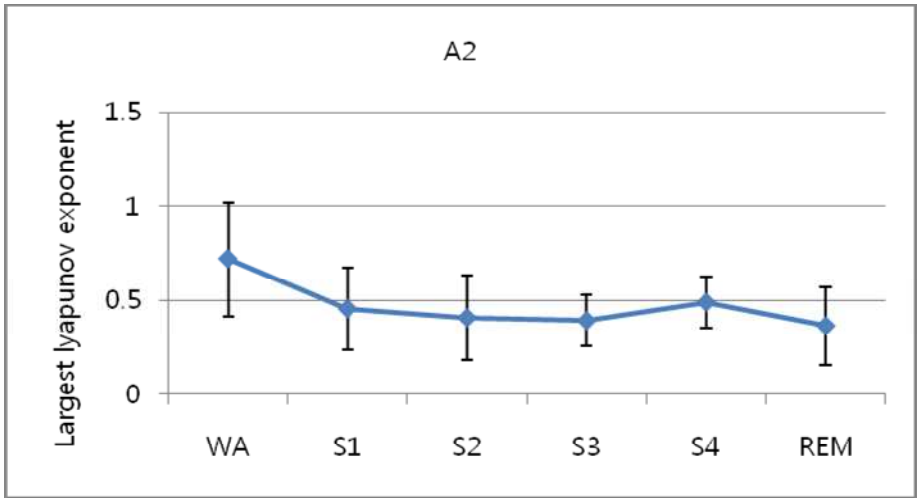
A2
Largest lyapunov exponent
1.5
1
0.5
0
WA
S1
S2
S3
S4
REM

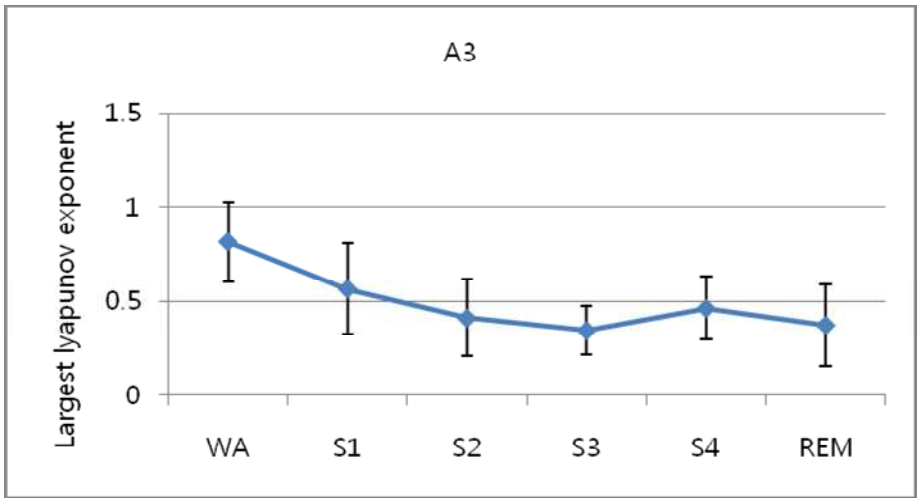
A3
Largest lyapunov exponent
1.5
1
0.5
0
WA
S1
S2
S3
S4
REM

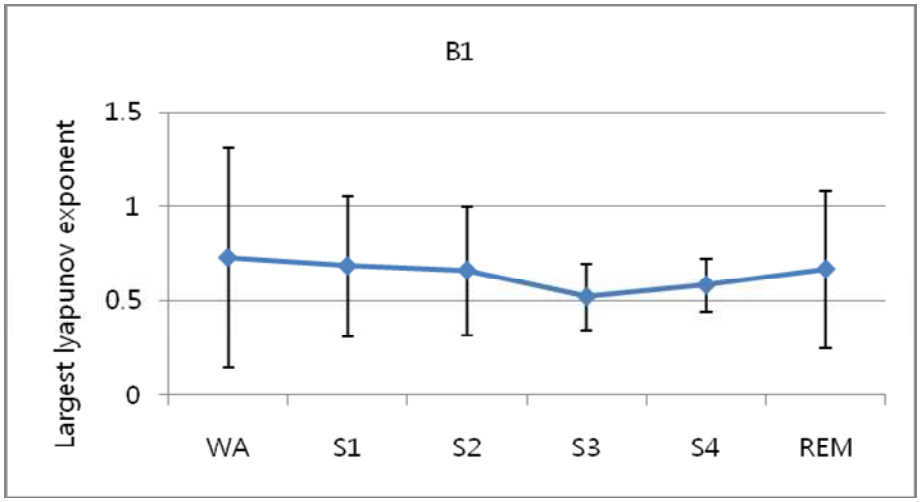
B1
Largest lyapunov exponent
1.5
1
0.5
0
WA
S1
S2
S3
S4
REM

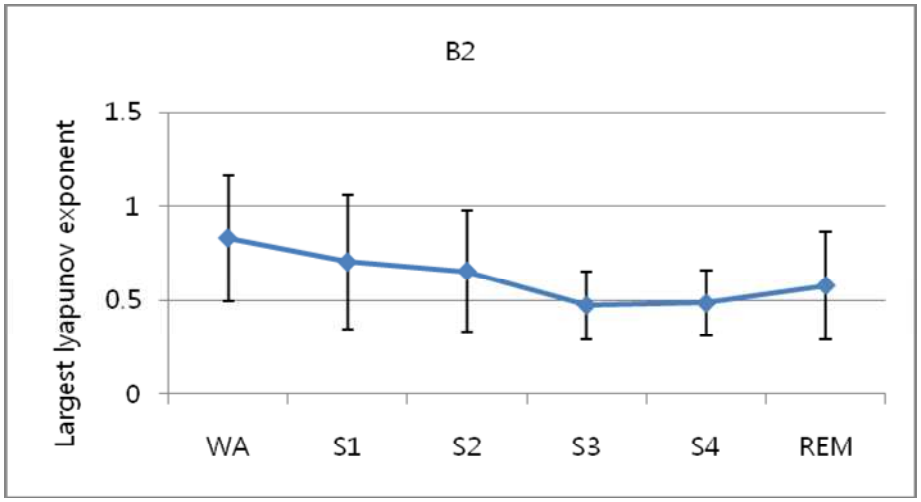
B2
Largest lyapunov exponent
1.5
1
0.5
0
WA
S1
S2
S3
S4
REM

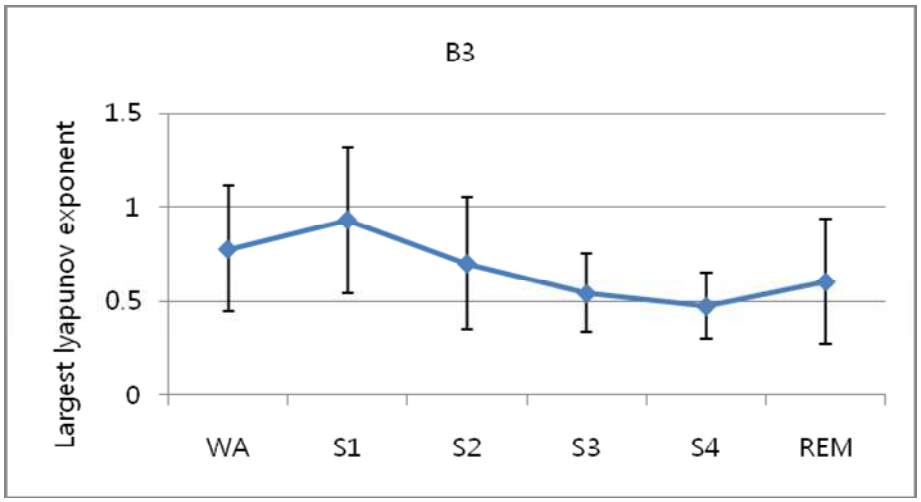
B3
Largest lyapunov exponent
1.5
1
0.5
0
WA
S1
S2
S3
S4
REM

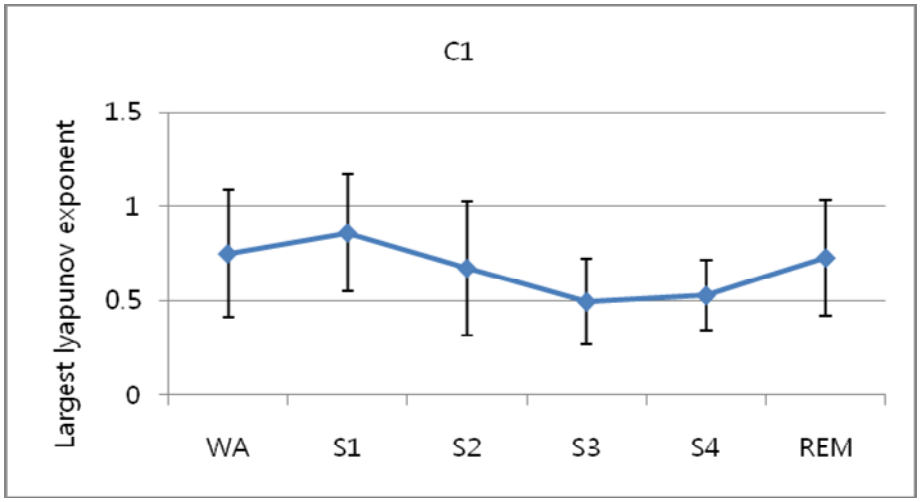
C1
Largest lyapunov exponent
1.5
1
0.5
0
WA
S1
S2
S3
S4
REM

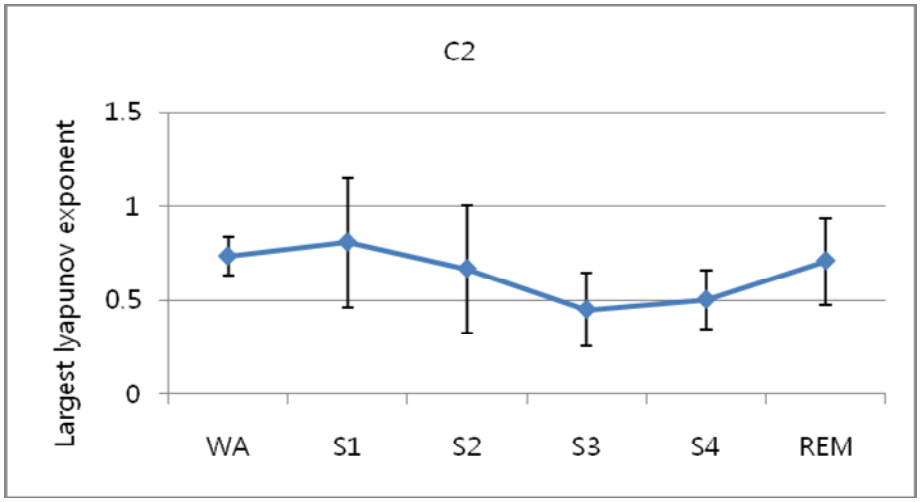
C2
Largest lyapunov exponent
1.5
1
0.5
0
WA
S1
S2
S3
S4
REM

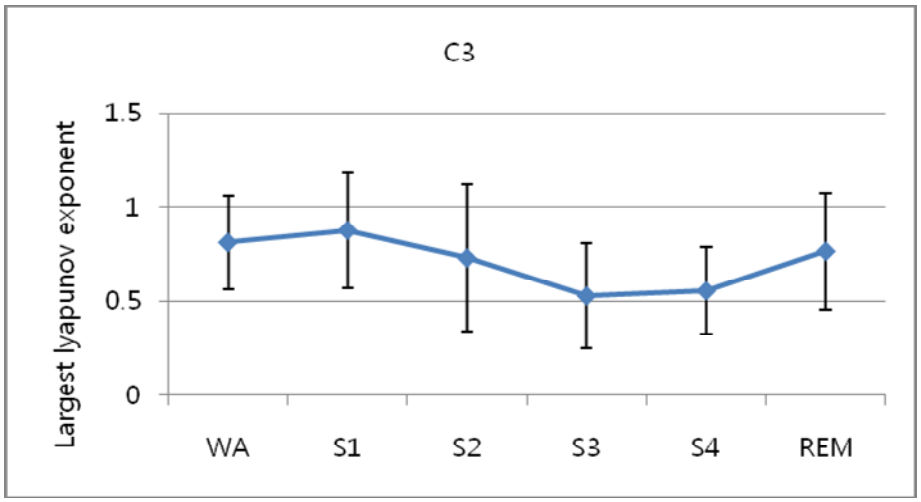
C3
Largest lyapunov exponent
1.5
1
0.5
0
WA
S1
S2
S3
S4
REM

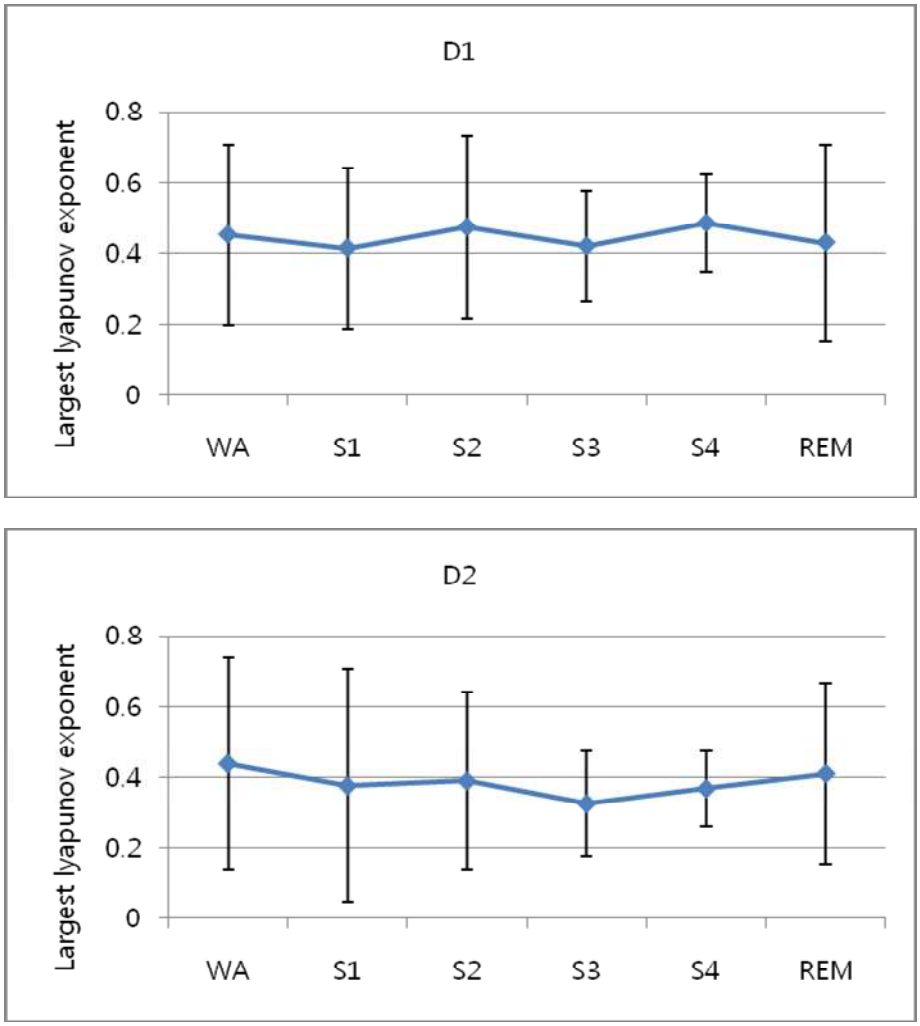

Figure 4.3 Mean and S.D. of L1 for WA stage, sleep stage 1, 2, 3, 4, and REM stage for each recording sets

Chapter *5*

5. Discussion

Recently, fuzzy inference systems and GAs have been used together to solve complex problems [17]. Fuzzy logic's uncertainty and GA's joint ability, they are together considered to be a "Soft-Computing" technique.

This thesis proposed a method of learning algorithms using a fuzzy inference system and a GA to classify sleep stages. Membership functions and fuzzy rules were optimized using GA operations corresponding to individual subjects.

Using the standard criteria, visual identification of sleep stages is difficult even for experts [20-22]. Identifying the percentage of a certain frequency range can lead to a questionable decision. As an example, in the standard method, a period that shows more than 20% and less than 50% delta activity scores as Stage 3, but is scored as Stage 2 when delta activity shows less than 20%. This thesis developed a fuzzy theory to distinguish between these uncertain parameters.

The results in Figure 5 show the variability between subjects' sleep EEG patterns, as well as similarities between the subjects. This result is consistent with previous research [8], and highlights individual differences in sleep patterns and stages between people. To correct the fuzzy classifier for individual subjects, a GA was used to optimize the parameters in the fuzzy classifier.

Power spectral analysis showed that individual frequency bands contained a number of factors which could allow it to be used alone for sleep staging. Figure 1 shows the patterns at different frequency ranges in different sleep stages that, after the calculation of relative power, were normalized based on a single EEG channel, C3-A2. These results indicate that sleep stages can potentially be scored using a single EEG signal only [23, 24].

The GFC performed comparably with conventional methods. Despite using a single signal and without any artifact rejection, the system demonstrated an accuracy of about 84.6% with a sensitivity of about 80% and good specificity in identifying four sleep stages (WA, SS, DS, and REM). The results found using the automated method are acceptable when compared with previous studies of automated sleep staging which correctly detected sleep stages approximately 75-85% of the time [3-5].

D2 and L1 for the entire sleep EEG per 30s epochs were calculated. The mean of D2 and L1 decreased from shallow sleep (Stage1 and 2) to deep sleep (Stage3 and 4) and only the D2 increased at REM stage. These results of D2 are generally consistent with the results reported by Roschke et al [25]. Because the neurons of the brain become more inactive as the person goes through from one sleep stage to the next sleep stage, until sleep stage 4, fewer number of neurons will be available for processing the information, and as a result the D2 and L1 fall. But in REM stage, the neurons become active as a result the D2 rise. Individual differences were also found in chaotic analysis. D2 and L1 respectively and displayed similar patterns between intra-subjects.

References

[1] A. Rechtschaffen, A Kales (Eds.), A manual of standardized Terminology, Techniques, and Scoring System for Sleep Stages of Human Sleep, Brain Information Service/Brain Research Institute, UCLA, Los Angeles, 1968.

[2] T. Penzel, R. Conradt, Computer based on sleep recording and analysis, Sleep Medicine Reviews, 4 (2) (2000) 131-148.

[3] T. Watanabe, K. Watanabe, Noncontact Method for Sleep Stage Estimation, IEEE Trans. Biomed. Eng. 51 (10) (2004) 1735-1748.

[4] A. Flexer, G. Gruber, G. Dorffner, A reliable probabilistic sleep stager based on single EEG signal, Artificial Intelligence in Medicine, 33 (2005) 199-207.

[5] J. Virkkala, J. Hasan, A. Varri, S.L. Himanen, K. Muuler, Automatic sleep stage classification using two-channel electro-oculography, Journal of Neuroscience Methods, 166 (2007) 109-115.

[6] H.P.A. Van Dongen, K.M. Vitllaro, D.F. Dinges, Individual differences in adult human sleep and wakefulness: Leitmotif for a research agenda, Sleep, 28 (4) (2005) 479-496.

[7] A.M. Tucker, D.F. Dinges, H.P.A Van Dongen, Trait interindividual differences in the sleep physiology of healthy young adults, J. Sleep. Res. 16 (2007) 170-180.

[8] J. Buckelmuuller, H.P. Landolt, H.H. stassen, P. Achermann, Trait-like individual differences in the human sleep electroencephalogram, Neuroscience, 138 (2006) 351-356.

[9] C.J. Stam, Nonlinear dynamical analysis of EEG and EMG: review of an emerging field, Clinical neurophysiology 116 (2005), 2266-2301

[10] E.H. Mamdani, S. Assilian, An experiment in linguistic synthesis with a fuzzy logic controller, International Journal of Man-Machine Studies, 7 (1) (1975) 1-13.

[11] L.A. Zadeh, Fuzzy sets, Information and control, 8 (1965) 338-353.

[12] A. M. Faser, H. L. Swinney, Independent coordinates for strange attractors from mutual information, Physical Review A, 33 (1986), 1134-1140

[13] M. B. Kennel, R. Brown, H. D. I. Abarbanel, Determining embedding dimension for phase-space reconstruction using a geometrical construction. Physical Review A, 45 (1992), 3403-3411

[14] P. Grassberger, I. Procassia, Measuring the strangeness of strange attractors, Physica D, 9 (1983), 189-208

[15] M. T. Rosenstein, J. J. Collins, and C. J. DeLuca, A practical method for calculating largest Lyapunov exponents from small data sets, Physica D: Nonlinear Phenomena, Issue 1-2 (65) (1992), 117-134

[16] J.H. Holland, Adaptation in Natural and Artificial Systems, University of Michigan Press, Ann Arbor, MI, 1975.

[17] E. Zhou, A. Khotanzad, Fuzzy classifier design using genetic algorithm, Pattern Recognition 40 (2007) 3401-3414.

[18] A. Arslan, M. Kaya, Determination of fuzzy logic membership functions using genetic algorithms, Fuzzy Sets and Systems, 118 (2001) 297-306.

[19] A. Roychowdhury, D.K. Pratihar, N. Bose, K.P. Sankaranarayanan, N. Sudhahar, Diagnosis of the diseases-using a GA approach, Information Sciences, 162 (2004) 105-120.

[20] Y.D. Kim, M. Kurachi, M. Horita, K. Matsuura, Y. Kamikawa, Agreement of Visual Scoring of sleep stages among Laboratories in Japan: Effect of a Supplementary Definition of Slow Wave on Scoring of Slow Wave Sleep, The Japanese Journal of Psychiatry and Neurology, 47 (1) (1993) 91-97.

[21] R. Norman, I. Pal, C. Stewart, J. Walseleben, D. Rappaport, Interobserver agreement among sleep scorers from different centers in a large dataset, Sleep, 23 (7) (2000) 901-908.

[22] F. Poree, A. Kachenoura, H. Gauvrit, C. Morvan, G. Carrault, L. Senhaji, Blind source separation for ambulatory sleep recording, IEEE Trans. Inf. Technol. Biomed. 10 (2) (2006) 293-301.

[23] M. C. Cabrera, Z. M. Torres, Y. R. Portilla, M. A. Guevara, Poer and coherent oscillations distinguish REM sleep, stage 1 and wakefulness, International Journal of Psychophysiology 60 (2006) 59-66

[24] R. Agarwal, J. Gotman, Computer-Assisted Sleep Staging, IEEE, Trans. Biomed. Eng. 48 (12) (2001) 1412-1423

[25] J. Roschke, J. B. Aldenhoff, A non-linear approach to brain function: Deterministic chaos and sleep EEG, Sleep, 15 (2) (1992), 95-101

국문요약

뇌파 기반 수면평가를 위한 Genetic Fuzzy Classifier 알고리즘 개발 및 비선형 분석

지금까지 수면다원검사는 1968 년에 정리된 R-K 기준을 기반으로 전문의가 직접 눈으로 보고 판단하는, 장시간의 작업을 필요로 하는 검사로 진행되어 왔다. 그러나 R-K 기준을 적용하기 위해서는 여러 전극을 두피와 얼굴 주위에 부착 해야 하기 때문에 일상의 수면을 유도하기가 어렵고, 수면단계를 나누는 기준이 명확하지 않아 전문가들 사이에서도 높은 정확도를 보여주지 못하고 있다. 이러한 근본적인 문제점을 개선하기 위하여 컴퓨터를 기반으로 수면다원검사를 하는 여러 방법들이 제안되고 있으나, 아직까지도 R-K 기준을 대체할만한 성능을 보여주지 못하고 있다.

따라서, 본 연구에서는 한 채널의 뇌파를 이용하여 개인의 수면 특성에 맞는 컴퓨터 기반 수면평가 알고리즘을 디자인하는 새로운 방법을 제안 함으로서, R-K 기준의 단점을 보완하고 기존의 컴퓨터 기반 수면평가 알고리즘의 성능을 향상시키고자 하였다. 이를 위하여 불분명한 수면단계를 구분하기 위한 목적으로 퍼지추론 시스템을 적용하였으며, 유전자알고리즘을 이용하여 퍼지추론 시스템의 소속함수와 퍼지규칙을 개인에게 최적화시켰다. 그 결과 본 연구에서 제안한 알고리즘은 수면단계를 4 단계로 구분하는데 약 84.6%의 정확도를 보였다.

또한, 뇌파를 주파수 대역별로 분석하여 개인별 수면단계의 특성 차이를 확인할 수 있었다. 그리고 비선형 분석방법인 카오스 분석을 적용하여 수면단계에 따른 차원의 복잡성과 초기의 민감성을 분석하여, 깊은 수면으로 갈수록 상관차원과

리아푸노프 지수가 낮아지고, REM 단계에서는 상관차원 값이 증가하는 현상이 나타나는 것을 확인하였다.

핵심이 되는 말 - 뇌파, 수면다원검사, 퍼지추론, 유전자 알고리즘, 카오스, 비선형 분석, 상관차원, 리아푸노프 지수